Medicinal mushrooms affect metabolic pathways in Trachea, bronchus, and lung cancer.

A Thesis

submitted to

Indian Institute of Science Education and Research Pune in partial fulfilment of the requirements for the BS-MS Dual Degree Programme

by

Prashant Kumar

Indian Institute of Science Education and Research Pune

Dr. Homi Bhabha Road,

Pashan, Pune 411008, INDIA.

Date: April, 2025

Under the guidance of

Supervisor: Dr. Medhavi Vishwakarma

Department of Bioengineering, Indian Institute of Science, Bengaluru

From May 2024 to Mar 2025

INDIAN INSTITUTE OF SCIENCE EDUCATION AND RESEARCH PUNE

Certificate

This is to certify that this dissertation entitled **"Medicinal mushrooms affect metabolic pathways in Trachea, bronchus, and lung cancer"** towards the partial fulfillment of the BS-MS dual degree programme at the Indian Institute of Science Education and Research, Pune represents work carried out by Prashant Kumar at the Indian Institute of Science Bengaluru under the supervision of **Dr. Medhavi Vishwakarma**, Department of Bioengineering, during the academic year 2024-2025.

Dr. Medhavi Vishwakarma

Committee:

Name of your Guide: Dr. Medhavi Vishwakarma

Name of Your TAC: Dr. Nagaraj Balasubramanian

This thesis is dedicated to my family, mentors, and loved ones, whose support and guidance have been the cornerstone of my academic and personal growth.

Declaration

I hereby declare that the matter embodied in the report entitled **“Medicinal mushrooms affect metabolic pathways in Trachea, bronchus, and lung cancer”** are the results of the work carried out by me at the Department of Biological sciences, Indian Institute of Science Education & Research (IISER) Pune, under the supervision of **Dr. Medhavi Vishwakarma**, and the same has not been submitted elsewhere for any other degree. Wherever others contribute, every effort is made to indicate this clearly, with due reference to the literature and acknowledgement of collaborative research and discussions.

PRASHANT KUMAR

20201146

Table of Contents

Contents

Abstract

Medicinal mushrooms offer significant anticancer benefits through immunomodulation, reduction of inflammation, direct cytotoxicity, and synergy with cancer therapies. Studies suggest that incorporating medicinal mushrooms into diets or treatments may enhance cancer prevention and support ongoing therapies. However, a mechanistic understanding of how medicinal mushrooms modulate metabolic pathways to affect cancer cell growth remains unclear. In this study, we use bio-active extracts of two edible and medicinal mushrooms, *Pleurotus Osteratus* and *Ganoderma Lucidium*, which have previously demonstrated anti-cancer properties, and delineate metabolic pathways that are affected in the cancer cell line of the Lung (A549), and the healthy airway epithelial cells (Beas2b). By measuring biochemical parameters such as intracellular ROS levels and altered energy metabolism, we show that in cancer cells treated with *P. Osteratus* and those treated with *G. Lucidium*, ROS levels are reduced, and glucose metabolism is impaired. There is a difference in these parameters, how mushrooms affect Beas2b cells. To mimic the in-vivo architecture of cancer, we performed these experiments in 3D cancer spheroids cultured in low attachment well plates, and our results show similar trends as cells in 2D monolayers. To access cell growth and morphological changes, we aim to perform immunostaining with actin and Caspase-8 staining, in both 2D monolayer cultures and 3D spheroid cultures treated with mushrooms.

Acknowledgments

I would like to express my gratitude to Dr. Medhavi Vishwakarma for allowing me to work under her guidance. Her constant support, invaluable insights, and unwavering faith in me have shaped my academic journey. She has been the best Principal Investigator (PI) I could have asked for, allowing me the freedom to explore, make mistakes, and learn from them with kindness and humility. Her mentorship has been a cornerstone of my growth, both as a researcher and as an individual.

I am also immensely grateful to Prof. K.V. Venkatesh from IIT Bombay for his collaboration on this project. His inputs and guidance have significantly enriched the quality of my work and broadened my perspective.

This research was made possible through a collaborative partnership with MetFlux Research, whose generous provision of reagents, resources, and technical expertise bridged the gap between academic inquiry and industrial application. Their support was instrumental in scaling key experiments and ensuring translational relevance.

My heartfelt thanks go to all the members of EMLAB at IISc Bengaluru for their support and camaraderie. Special thanks to Michelle for her assistance with experiments and for enduring my sarcasm with patience; to Varnit for his invaluable inputs, late-night tissue culture struggles, and constant help throughout my thesis; to Ketaki and Aswin for being wonderful friends and making my time in the lab enjoyable; and to Amrapali, Sindhu, Sutha, Chandan, Bhargavi, Lakshmi, and Tanishq for their constant motivation, laughter, and support. I would also like to mention Arjun from Sanhita's lab for his help with the Spectrofluorometer and his availability at absurd hours.

I extend my gratitude to the cricket and carrom community at IISc Bengaluru for providing a much-needed escape from the rigors of research and for fostering a sense of belonging.

I would like to acknowledge Dr. Nagaraj Balasubramanium for believing in me during the nascent phase of my research career. His permission to work in the Adhesion Lab at IISER Pune allowed me to explore my interests in biology and cancer research. I am thankful to my mentor Antara for helping me nurture my skills, and to Tushar and Abhishek for being like friends in the lab and lightening the tensions with their

presence. My thanks also go to all the members of the Adhesion Lab for their support and encouragement.

The motivation to pursue basic science was instilled in me by two of my faculty members at PCP Sikar, Dr. Rakesh Ruhela and Dr. Umesh C. Pachouri. They sowed the seed of curiosity and passion in me, and this thesis is a result of their inspiration.

I would also like to mention the cricket and carrom community at IISER Pune for being my source of joy and relaxation outside of research. Special thanks to Amrit, Bharat, Manali, Suyog, Nayana, and Pallav for the unforgettable carrom memories, and to the IISER Premier League cricket teams - Master Batters, TEAM-X, and Gardening Team for the camaraderie and fun on the field. Also, I would like to thank my friends, Prabhat, Shresth, Paritosh, Nandeesh, Aniket, Rafael, Kavan, seniors, and juniors at IISER Pune for their unwavering support, encouragement, and love throughout this journey.

I acknowledge the Kishore Vaigyanik Protsahan Yojana (KVPY) for their financial support through the scholarship, which empowered me to pursue research without constraints.

Above all, I owe everything to my pillars of strength, my family. Their emotional encouragement, financial sacrifices, and physical presence during every high and low gave me the resilience to persevere. This achievement is as much theirs as it is mine.

This thesis would not have been possible without their belief in me.

Chapter 1. Introduction

Trachea, bronchus, and lung cancer statistics and limited therapies:

The International Agency for Research on Cancer (IARC) published in 2022, 12.42% (2,480,675) of the 19,976,499 recorded cases of cancer globally were caused by trachea, bronchus, and lung cancers, By causing 18.1% of all the cancer related deaths, these are the leading cause of deaths due to cancer worldwide (1). Regional variations in disease burden are evident in high age-standardized prevalence rates (ASPR) in high sociodemographic index (SDI) areas like East Asia (43.41 cases per 100,000 population) and high-income North America (37.21 cases per 100,000 population), while Western Sub-Saharan Africa had the lowest ASPR (3.68 cases per 100,000 population). There was a marginal increase in global ASPR of 0.09 cases per 100,000 population between 1990 and 2021. Still, trends were found to be declining in countries like high-income North America and Southern Latin America (Figure 1. a) (2), indicating lifestyle as a major factor, highlighting of the implementation of effective prevention measures. Furthermore, cancer cases are projected to increase to an alarming 35 million by 2050 (3).

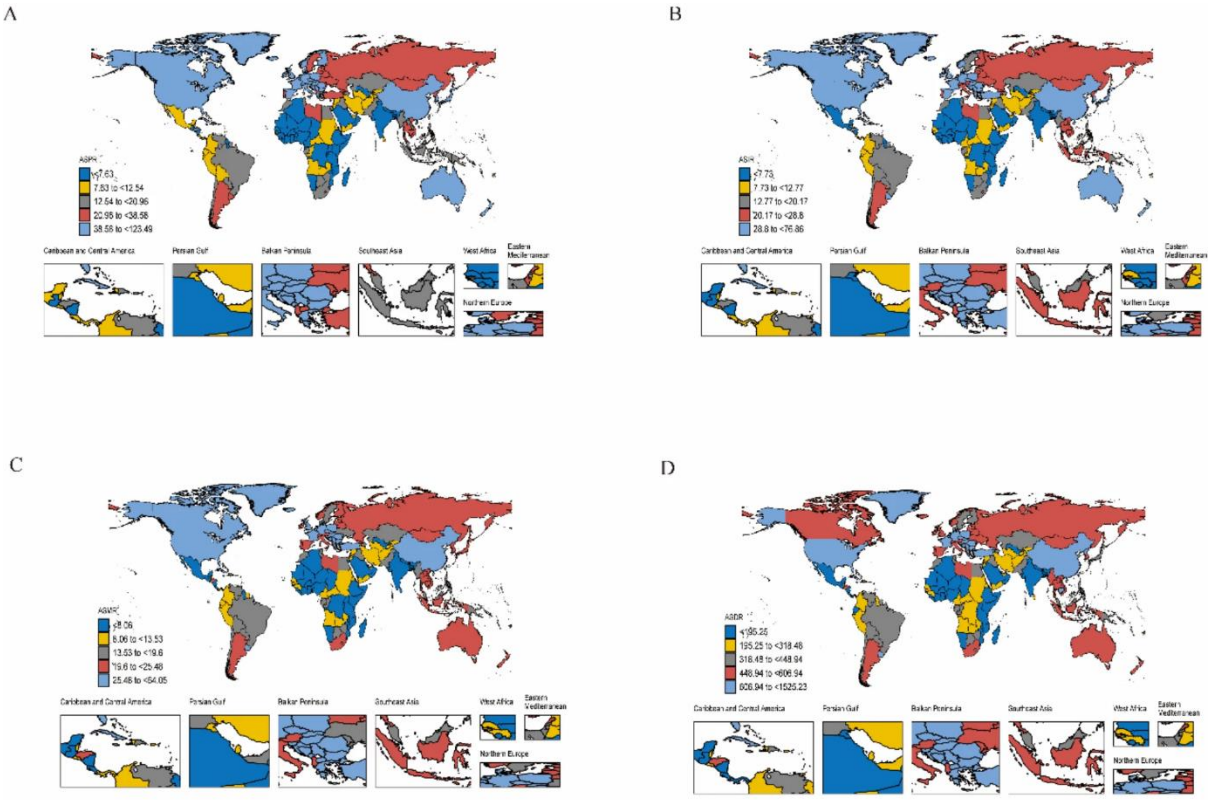

Figure 1. a. TBL distribution of disease burden in 2021 globally. (A) Age-standardized prevalence rates (B) Age-standardized incidence rates (C) Age-standardized mortality rates (D) Age-standardized (Disability-adjusted life years) DALYs rates.

Standard therapeutic methods for cancer therapy include surgical intervention, radiotherapy, chemotherapy, targeted therapy, and immunotherapy. While these approaches have saved countless lives, they are expensive, often unavailable, and often accompanied with severe side effects. Side effects like gastrointestinal disturbances, haemorrhagic cystitis, hair loss, cardiovascular and neurological toxicities (4) not only complicate recovery but also negatively impact patients' quality of life. Lifestyle and dietary habits along with environmental risk factors and genetics makes a person susceptible to cancer. It is especially true in case of trachea, bronchus, and lung cancer, therefore improving dietary habits and lifestyle offers should be effective in mitigating the risk of oncogenesis. As cancer development is a gradual multi-stage process that unfolds over an extended period (5), prioritizing prevention strategies may prove to be a more effective approach for managing and ultimately eradicating cancer.

Natural Products as an alternative:

In recent years, the limitations of conventional cancer therapies, such as modest treatment outcomes and severe side effects, have underscored the need for alternative and integrative approaches. Dietary compounds, proven to manage chronic diseases, are being now explored as anti-cancer agents. Bioactive reagents extracted from dietary compounds can have anti-cancer properties (6). They also enhance treatment efficacy while reducing adverse effects. Among natural products, edible and medicinal mushrooms stand out as rich sources of bioactive compounds and nutraceuticals. Research demonstrates that mushrooms can boost the effectiveness of chemo- or radiotherapy while minimizing side effects (7), ultimately improving patients' quality of life.

Edible (*Pleurotus ostreatus*, Cordyceps militaris) and medicinal (Ganoderma lucidum) mushrooms are rich sources of bioactive reagents and nutraceuticals with reported antioxidant, antidiabetic, and antitumor effects (7). Research demonstrates that

mushrooms can boost the effectiveness of chemo- or radiotherapy while minimizing side effects (8).

Pleurotus ostreatus the oyster mushroom, (Figure. 2.a.) belonging to the Pleurotacae family of the Kingdom Fungi and is the second most cultivated mushroom.


Figure. 2.a. *Pleurotus ostreatus* b. *Pleurotus ostreatus* extract

P. Ostreatus in their fruiting bodies has different bioactive and phenolic compounds [9] containing higher content of elements like Cu, Fe, K, Mg, P, Zn, and Na [10]. Different extracts of *P. Osteratus* (Figure 2.b.) have been reported to possess anticancer properties. Water-soluble extracts of *P. Ostreatus* have significant cytotoxicity and induced apoptosis in human prostate cancer cells androgen-independent PC-3 [11]. *Pleurotus ostreatus* shows significant antioxidant activity, as it can scavenge free radicals, reduce ferric ions, and cause hydrogen peroxide inactivation. The findings prove that *Pleurotus ostreatus* is a significant source of natural antioxidants, showing its potential in treating diseases caused by oxidative stress (12).

Ganoderma lucidum, (Figure 3.a.) commonly known as Reshi, belongs to the *Ganodermataceae* family of the Kingdom Fungi. The fruiting bodies of Reshi extracts (Figure 3.b.) consist of polysaccharides, triterpenes, and beta-glucan with known pharmacological activities. In a time- and dose-dependent manner, breast cancer


Figure. 3.a. *Ganoderma lucidum* *b. Ganoderma lucidum extract*

cells MCF-7 were treated using Se-GLPs causing decreased cell viability and the cell cycle arrest at the sub-G1 phase [13]. Findings are being carried out for different extracts in varying compositions as a potent medicine for cancer, diabetes, and other diseases catering to its anticancer, antioxidant, antibacterial, and antiviral effects. *Ganoderma lucidum's* fruiting body extracts are good sources of phenolic compounds and triterpenoids. Extracts exhibit strong antiproliferative activities against various cancer cell lines. These bioactive compounds induce cancer cell apoptosis by multiple mechanisms, indicating their potential application in the treatment of breast, colorectal, and colon cancers. *G. lucidum* extracts exhibit a promising future for the treatment of oxidative stress-related diseases, particularly cancer (14).

Gaps in current research:

Firstly, while previous studies have highlighted the potential of individual mushroom extracts by evaluating cell viability and apoptosis induction, key metabolic markers like lactate production, glucose uptake, and reactive oxygen species (ROS) levels not evaluated. These markers are essential for understanding how mushrooms influence cancer cell metabolism, in the context of the Warburg effect. It is hallmark of cancer characterized by increased glycolysis and lactate production. Second, the specific molecular mechanisms by which bioactive compounds in mushrooms modulate cancer metabolism remain unclear, particularly the roles of glucose transporter GLUT1 and other metabolic regulators. Investigating such combinations could reveal enhanced therapeutic benefits, including improved efficacy and reduced side effects. Third, many studies rely on monolayer cultures, which do not fully recapitulate the complex 3D architecture and metabolic dynamics of *in vivo* tumors. Finally, the potential synergistic effects of combining extracts from different mushroom species have not been thoroughly explored.

Metabolic markers

ROS

Incomplete reduction of molecular oxygen generates Reactive oxygen species (ROS), a collective term includes the superoxide anion (O2), hydrogen peroxide (H2O2) and hydroxyl radical (OH). During anaerobic metabolism, ROS are generated as byproducts primarily in the mitochondria, endoplasmic reticulum (ER), peroxisomes, and plasma membrane. ROS has dual physiological roles, at low levels, acts as signalling molecules responsible for cellular processes, and at higher levels causes oxidative stress causing DNA damage, leading to cancer pathogenesis (15), diabetes, neurodegenerative disorders, and atherosclerosis. Electron leakage from complexes I and III of the electron transport chain in mitochondria produces superoxide ($O_2^{\bullet -}$), further enzyme superoxide dismutase (SOD) converts it to hydrogen peroxide (H_2O_2) Figure 4. (16,17,18). NADPH oxidases (NOX) also generate superoxide by transferring electrons to oxygen.

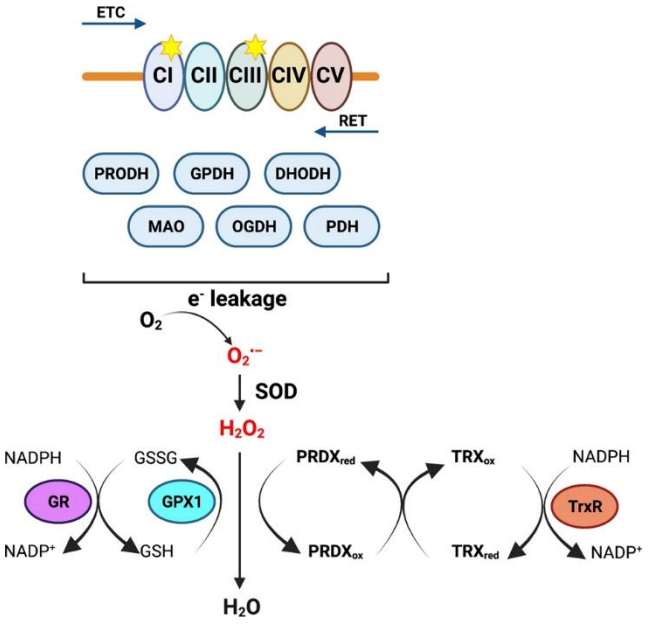

Figure 4. ROS generation: sources, enzymes, and pathway.

ER produces ROS during protein folding and cytochrome P450 activity (19), while peroxisomes generate ROS during fatty acid oxidation (20). External factors like UV radiation, pollutants, and tobacco smoke also contribute to ROS generation. Reactive Oxygen Species (ROS) have a dual role in cancer (Figure 5) (21). ROS at optimum levels stimulate tumor cell proliferation by activating pathways such as JNK, ERK, and NF-Kb (22). ROS induces DNA damage, mutations, and impaired repair at higher levels, leading to normal cell transformation into cancer cells (23). ROS also increases tumor invasion and metastasis by upregulating matrix metalloproteinases (MMPs) and stabilizing HIF-1α (24). Essential signaling pathways such as AKT, Wnt/β-catenin, and PI3K/AKT/mTOR are controlled by ROS, and thus are pivotal for cancer pathogenesis (25). At extreme levels, causing cell death.

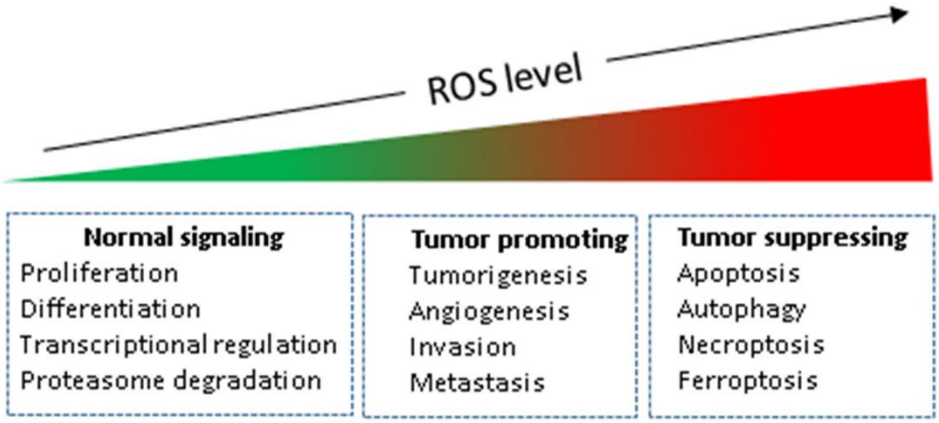

Figure 5. The role of ROS in cancer, transitioning from normal signaling to tumor promotion and suppression based on ROS levels.

Altered Energy Metabolism

Altered metabolism refers to changes in the way cells process nutrients to produce energy and biomolecules. In normal cells, metabolic processes are tightly regulated to achieve a balance between energy generation (by oxidative phosphorylation) and biosynthesis. In cancer cells, metabolic processes are altered to support rapid proliferation, survival, and growth even under hypoxia and nutrient starvation. Rewiring of glucose metabolism also referred to as the Warburg effect or aerobic glycolysis, is a characteristic of cancer, wherein cancer cells use glycolysis almost exclusively for energy generation regardless of the oxygen availability (26). This involves increased

glucose uptake, increased glycolysis, and lactate production, mediated through the overexpression of glucose transporters. Overexpression of hexokinase-2 and lactate dehydrogenase (LDH) enables cancer cells to rapidly produce ATP and supply intermediates for the pentose phosphate pathway. Pyruvate produced at the terminal step of glycolysis is oxidized to lactate rather than entering mitochondria for oxidative phosphorylation. Increased lactate production not only recycles NAD+ to sustain glycolysis but also generates acidic microenvironment assisting tumor invasion, metastasis, and immune evasion. Upregulation of glucose transporter GLUT1 is at the center of enabling this metabolic shift. By facilitating glucose uptake, GLUT1 enhances the elevated glycolytic rates observed in cancer cells, thereby allowing ATP production and biosynthetic processes necessary for cell growth. PI3K/AKT, MYC, and hypoxia-inducible factor 1α (HIF-1α) mediates GLUT1 overexpression, expressed in the tumor microenvironment (27). These changes enable cancer cells persist in stressful microenvironments, and become resistant to therapies (28). GLUT1 can thus be a potential therapeutic target as its inhibition interfere with cancer metabolism and suppress tumor growth.

Combination of extracts

The efficiency of mushroom extracts to elicit health responses greatly depends on the process of extraction and the solvent utilized. Water-based and ethanol-based solvents are widely used in extraction processes since they differ in polarity and are hence effective in isolating a range of phytochemical classes. Water-based solvents mainly extract phytochemicals with antioxidant activity, whereas ethanol-based solvents extract those with antimicrobial and anti-inflammatory activity (29,30). The combination of extracts from multiple solvents is an effective strategy to enhance the total efficacy of phytochemicals from mushrooms. This would not only be beneficial in achieving comprehensive extraction of phytochemicals, but the polar metabolites of water extracts may be complemented with the moderately polar and lipophilic compounds from ethanol extracts to produce an evenly balanced and highly effective blend with maximum antioxidant capacity (31), enhanced therapeutic effect (12). Optimization of extraction steps and blending of solvents will thus enable it to achieve

the greatest medicinal worth from mushrooms and ultimately establish the bases for the commercial development of functional foods, supplements, and medications which mitigate oxidative-stress related disease processes and other healthcare disorders.

Spheroids over monolayer culture

Cancer biology research and the establishment of successful therapeutic approaches have depended for a long time on conventional monolayer cell culture systems. Although these systems have yielded valuable insights into cellular behavior and drug sensitivity, they fail to accurately mimic the complex *in vivo* tumor microenvironment. Solid tumors are defined by complex cellular interactions, gradients of nutrients, and heterogeneous metabolic processes, which are unaccounted for in monolayer cultures. This shortcoming has driven the quest for physiologically relevant *in vitro* systems that accurately reflect the *in vivo* tumor microenvironment. Multicellular tumor spheroids (MCTS), or spheroids, are an intriguing three-dimensional (3D) cell culture model that closely replicates the structural and functional complexity of solid tumors. Spheroids recapitulate salient features of tumor biology, including cell-cell interactions, extracellular matrix (ECM) deposition, and the formation of nutrient and oxygen gradients, which lead to differentiated regions of proliferation, quiescence, and necrosis. Recent studies have also revealed dramatic differences in metabolic phenotypes between 2D and 3D cultures, highlighting the necessity to use spheroids to study cancer metabolism. These characteristics make spheroids a more appropriate model to study tumor metabolism, drug penetration, and efficacy of therapeutic agents.

The primary goal of this study is to delineate the metabolic pathways influenced by mushroom (*Pleurotus ostreatus* and *Ganoderma Lucidium*) extracts in lung cancer cell line A549 and to compare these effects with those in healthy cell line BEAS2B. airway epithelial cell line (BEAS-2B) cells. The experiments would be performed on both monolayer cultures and spheroid models. We will measure ROS levels, glucose uptake, lactate production, and GLUT1 expression, to provide a depth understanding

of how these mushrooms modulate cancer metabolism. Additionally, we will explore the synergistic effects of combining different extracts from these two mushroom species across varying concentrations. The research aims to provide a scientific basis for their use as a preventive and complementary treatment for cancer. This study was undertaken to address the growing need for low-toxicity, integrative approaches that can enhance the efficacy of conventional therapies while minimizing adverse effects, ultimately improving patients' quality of life.

Chapter 2. Methods and Materials

Mushroom extraction

P. Ostreatus Mushroom cultivation

P. Ostreatus mushroom was cultivated using Paddy straw as a substrate. The paddy straw was layered and spawned using P. ostreatus spawn in a polythene bag. The bag was kept at 25°C for 15 to 20 days in the dark for complete mycelation. The fully myceliated bags were then transferred to the growth room, providing 1500 lux light intensity for 12 hours with fresh air and humidity above 70%. After 5 to 10 days, mushrooms start to grow. The Fresh mushrooms were harvested at optimal maturity, ensuring the absence of any visible contamination.

Ganoderma Lucidium Mushroom cultivation

Ganoderma Lucidium (commonly known as Reishi Mushroom) cultivation was done using wheat bran as a substrate and sawdust as a supplement. To obtain a final moisture content of 65%, the substrate was mixed with water. The 1.5 kg of substrate was autoclaved, filled in polypropylene bags, and incubated at 121 °C for 2 hours. Then the bag was cooled to room temperature. The top layer spawning was done using *Ganoderma Lucidum* spawn and incubated at 25 °C for 1 month in the dark for complete mycelation. The fully myceliated bags were transferred to the growth room, providing 25 – 28 °C, 1500 lux light intensity for 12 hours with fresh air and humidity above 70%. After 5 to 10 days, a mushroom starts to grow. Fresh mushrooms were harvested at optimal maturity, which takes around 10 to 15 days, ensuring the absence of any visible contamination.

Mushroom Drying

Fresh mushrooms were dried using a Heat pump dryer set at 50°C for 8- 12 hours. The dried mushroom extracts (Figure 6.a. and b.) were subsequently ground into a fine powder using a laboratory grinder. To ensure uniform particle size, sieving of the *P. Ostreatus* mushroom powder was completed through a 60-mesh sieve.

Figure 6.a. Dry extracts of *Pleurotus ostreatus* b. Dry extracts of *Ganoderma lucidum*

Solvent Extraction Using Soxhlet Apparatus:

The weighed mushroom powder (100 g) was placed in a thimble made of filter cloth of 50 microns and loaded into the Soxhlet extractor (Figure 7).

Figure 7. Mushroom Extraction using the Soxhlet extractor.

Two sequential extractions were carried out: a) Ethanol Extraction: 2 L of ethanol was used as the solvent. The Soxhlet apparatus was operated at the solvent's boiling point, allowing continuous cycling of the solvent through the mushroom powder for 12 hours to ensure exhaustive extraction of ethanol-soluble compounds. b) Water Extraction: After ethanol extraction, the same mushroom powder was subjected to water

extraction using 2 L of distilled water. The Soxhlet extraction was continued under similar conditions for another 12 hours.

Concentration of Extracts:

The ethanol and water extracts obtained from the Soxhlet apparatus were separately collected. The extract was vacuum filtered (Figure 8. b.) using a Whatman filter. Using a rotary evaporator (Figure 8. a..) under reduced pressure, each extract was then concentrated at temperatures not exceeding 45°C for ethanol extracts and 55°C for water extracts to prevent the degradation of heat-sensitive bioactive compounds.

Figure 8. a. Rotary evaporator b. Vacuum Filtration

Drying of Concentrated Extracts:

The concentrated extracts were dried in a hot air oven at 50°C to achieve a constant weight. This ensured complete removal of residual solvents, resulting in dry ethanol and water extracts.

Preparation of Final Extract Solutions:

For analytical purposes, final extract solutions were prepared as follows: a) Ethanol Extract Solution: To prepare a stock solution with a concentration of 10 mg/mL, the dried ethanol extract was dissolved in ethanol. b) Water Extract Solution: Similarly, the dried water extract was dissolved in water to achieve a final concentration of 10 mg/mL.

Monolayer culture

BEAS2B

The human bronchial epithelial cell line BEAS-2B (InStem, Bangalore, India). Cells were cultured in Dulbecco's Modified Eagle Medium (DMEM) supplemented with 10% fetal bovine serum (FBS) (ThermoFisher Scientific), 1% P-S (penicillin-streptomycin), and 2 mM L-glutamine in a T-25 flask at 37°C and 5% CO_2. Cells were detached and sub-cultured every 3-4 days at approximately 75-80% confluence using 0.25% trypsin-EDTA. The cell line tested negative for mycoplasma contamination.

A549

The human lung adenocarcinoma cell line A549 (ATCC), gifted from Ashok M Raichur, Professor at the Department of Materials Engineering, Indian Institute of Science (IISc), Bengaluru. Cells were cultured in DMEM (ThermoFisher Scientific) supplemented with 10% FBS (ThermoFisher Scientific), 1% P-S, and 2 mM L-glutamine in a T-25 flask at 37°C and 5% CO_2. Cells were detached and sub-cultured every 3-4 days at approximately 75-80% confluence using 0.25% trypsin-EDTA. The cell line tested negative for mycoplasma contamination.

Spheroids

For spheroid formation, 15-30 × 10^3 A549 cells were seeded per well in U-bottom low-attachment 96-well plates (ThermoFisher Scientific) in 200 µL of complete DMEM. Plates were centrifuged at 500 g for 5 minutes to promote cell aggregation and then incubated at 37°C and 5% CO_2. Spheroids were allowed to form over 72 hours. Spheroid size and morphology were assessed using phase contrast microscopy.

Detection of intracellular reactive oxygen species (ROS) generation

Monolayer and spheroid cultures in a 96-well plate and a U-shaped low attachment 96-well plate, respectively, were washed with PBS and treated with 5 µM of 200 µL Dihydrorhodamine 123 (ThermoFischer Scientific) for 1 h, 37 °C, light-protected. The cells were then washed with PBS. Fluorescence detection was done using a plate reader (Biotek synergy H1 Microplate Spectrofluorometer) using excitation and emission wavelengths set at 485±20 nm and 528±20 nm, respectively.

Protein Quantification Using BCA Assay

Protein content was determined using the BCA Assay Kit (ThermoFisher Scientific). The BCA assay is based on the reduction of Cu^{2+} to Cu^{+} using proteins in an alkaline medium, followed by the colorimetric detection of Cu^{+} using bicinchoninic acid (BCA).

Sample Preparation

Cells were lysed using RIPA buffer (ThermoFisher Scientific) and protease inhibitor cocktail (Sigma Aldrich). The lysate samples were incubated at 4°C for 30 minutes.

BCA Assay Protocol

A standard curve was prepared using bovine serum albumin (BSA) provided in the kit, as per the manufacturer's instructions. The BCA working reagent was prepared by mixing reagent A with reagent B in a 50:1 ratio (v/v) as per the manufacturer's instructions. Aliquots of 25 µL of each standard or sample were added to a 96-well plate (ThermoFisher Scientific) in triplicate. Then, 200 µL of the BCA working reagent was added to each well. The plate was incubated at 37°C for 30 minutes, and absorbance was measured at 562 nm using a microplate reader (Biotek synergy H1 Microplate Spectrofluorometer). ROS readings were normalized to the protein concentration obtained using the BCA Assay.

Protein Extraction and Quantification

Sample Preparation

Cells were lysed using 1× Laemmli buffer (HiMedia) containing 10% β-mercaptoethanol and heated at 95°C for 10 minutes to denature the proteins. Equal amounts of lysate sample (30 µg per lane) were loaded in an SDS-polyacrylamide gel.

SDS-PAGE and Western Blotting

SDS-PAGE (5% stacking gel and 12.5% resolving gel) was performed at 30 V (15 mA current) for the first 30 min to get proteins into the resolving gel and then at 120 V for the next 1.5 hrs (till dye flows out of polyacrylamide gel) with running buffer (containing 100 ml 10X Tris-glycine, 10 ml 10% SDS and 890 ml distilled water). Proteins were transferred to a PVDF membrane for 2 hrs in chilled transfer buffer (Transfer buffer composition: 100 ml 10X Tris-glycine, 100 ml methanol, 800 ml distilled water, and 1 ml 10% SDS).

Antibody Incubation

Blocking of the membrane was done with 5% non-fat dry milk in TBST (Tris-buffered saline with 0.1% Tween-20) for 1 hour at RT. The membrane was incubated overnight at 4°C with a primary antibody against GLUT1 Polyclonal Antibody (ThermoFischer Scientific) diluted 1:1000 in 5% BSA in TBST. The membrane was washed three times for 10 minutes each with TBST and then incubated with a horseradish peroxidase (HRP)-conjugated secondary antibody (Jackson Immuno Research) at a dilution of 1:5000 in 5% non-fat dry milk in TBST for 1 hour at room temperature. The membrane was washed three times for 10 minutes each with TBST.

Detection and Imaging

As per the manufacturer's instructions, protein bands were visualized using a LAS 4000 imaging system with substrate and luminol (in a 1:1 ratio) solution.

Immunofluorescence Assay

Spheroids were washed with PBS and then fixed, permeabilized, and blocked using 4% paraformaldehyde, 1% Triton X-100, and 2% FBS + 2% BSA, respectively. It was then followed by primary antibody incubation with Rabbit monoclonal against E-cadherin (1:500) at 27 °C overnight. Appropriate secondary antibody was used: Anti-rabbit Alexa Fluor 488 (1:250) at 27 °C overnight. Subsequently, it was stained for F-actin using rhodamine 594 (1:250) and counterstained with DAPI (1:500).

Statistical analysis

ROS data was divided by the normalized protein concentration obtained using BCA assay as per the manufacturer’s instructions. Data was analyzed, graphs were plotted in Prism GraphPad.

Chapter 3. Results

Mushroom dilution in solvents

Mushroom extracts were provided by a collaborator and standardized at a 10 mg/mL concentration. Preliminary experiments were performed to identify the optimal concentrations for cell viability and biological activity. 4 µg/mL, 8 µg/mL, and 16 µg/mL concentrations were chosen for further experiments on the effects on cell viability because these concentrations were not cytotoxic to BEAS-2B cells. Both mushroom species, *Pleurotus ostreatus* and *Ganoderma lucidum,* were screened, both of which were extracted using two solvents: aqueous and ethanol. The variables screened were: *Pleurotus ostreatus* in ethanol, *Pleurotus ostreatus* in aqueous, *Ganoderma lucidum* in ethanol, *Ganoderma lucidum* in aqueous, *Pleurotus ostreatus* in ethanol + aqueous, and *Ganoderma lucidum* in ethanol + aqueous. But the significant reduction in ROS content was seen for ethanol and aqueous extracts supplemented for both varieties of mushrooms. They were chosen for the next experiments as they had better antioxidant activity than the single extracts.

ROS in Beas2b monoculture

The effect of *Pleurotus ostreatus* (ethanol + water extracts) on ROS level was assessed by measuring ROS normalized to protein concentration. From Figure 9., the highest ROS level was recorded from the control group (Media). *Pleurotus ostreatus* extract treatment with 4 µg/mL and 8 µg/mL was seen to significantly reduce ROS level, with both groups recording nearly a 50% reduction from the control. Statistical analysis revealed a highly significant decrease ($p < 0.01$) at these concentrations. The treatment group of 16 µg/mL revealed a minimal increase in ROS above 4 µg/mL and 8 µg/mL, but was significantly less compared to the control ($p < 0.05$). These results

show that *Pleurotus ostreatus* extracts have a dose-dependent effect on ROS levels, with maximum antioxidant activity at 8 µg/mL.

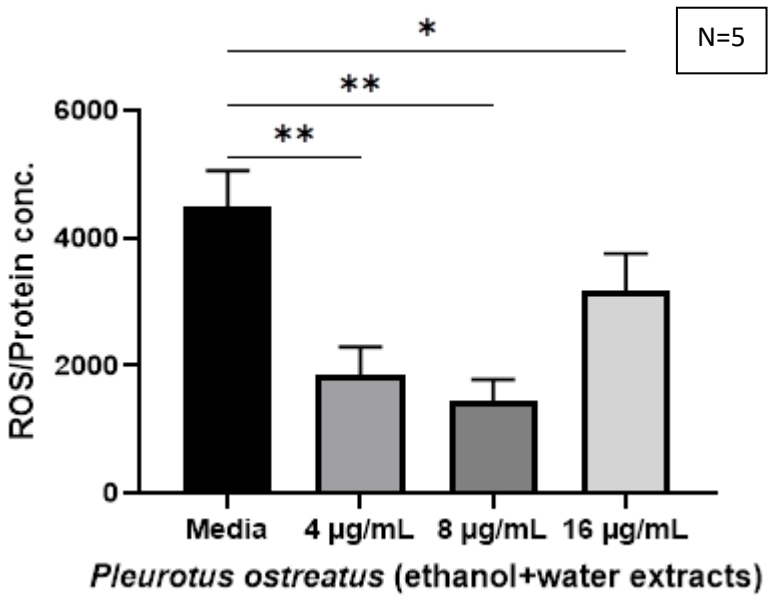

Figure 9. *Pleurotus Ostreatus* (ethanol + water extracts) in BEAS2B monolayer culture. ROS/ Protein conc. plotted against Media, 4 µg/mL, 8 µg/mL, and 16 µg/mL conc. of Pleurotus Ostreatus (ethanol + water extracts).

The effect of *Ganoderma lucidum* (ethanol + water extracts) on ROS levels was assessed by measuring ROS normalized to protein concentration. From Figure 10, the highest ROS level was recorded in the control group (Media). Treatment with *Ganoderma lucidum* extract at 4 µg/mL and 8 µg/mL significantly reduced ROS levels, with both groups showing more than 50% reduction from the control. Statistical analysis revealed a highly significant decrease ($p < 0.01$) at these concentrations. The 16 µg/mL treatment group exhibited an increase in ROS levels compared to the 4 µg/mL and 8 µg/mL groups, but was not significantly different from the control (ns). These results indicate that *Ganoderma lucidum* extracts exhibit antioxidant effects at lower concentrations (4 µg/mL and 8 µg/mL), but their efficacy diminishes at higher concentrations (16 µg/mL).

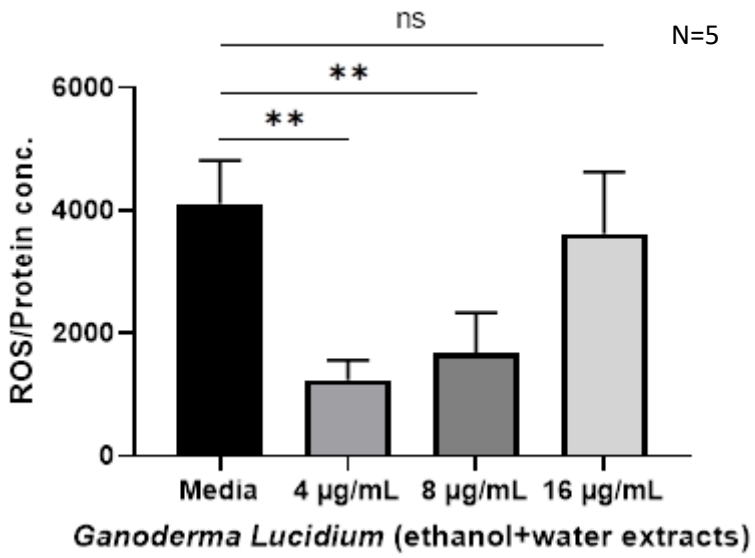

Figure 10. *Ganoderma lucidum* (ethanol + water extracts) in BEAS2B monolayer culture. ROS/ Protein conc. plotted against Media, 4 µg/mL, 8 µg/mL, and 16 µg/mL conc. of *Ganoderma lucidum* (ethanol + water extracts).

ROS in A549 monoculture

The effect of *Pleurotus ostreatus* (ethanol + water extracts) on ROS levels was assessed in A549 cells by measuring ROS normalized to protein concentration. As shown in Figure 11, the highest ROS levels were recorded in the control group (Media). Treatment with *Pleurotus ostreatus* extract at 4 µg/mL, 8 µg/mL, and 16 µg/mL significantly reduced ROS levels in a dose-dependent manner. The 4 µg/mL group showed a notable decrease, while 8 µg/mL and 16 µg/mL exhibited a further reduction, with 16 µg/mL displaying the lowest ROS levels. Statistical analysis confirmed a highly significant reduction ($p < 0.001$) across all treatment groups compared to the control. These findings suggest that *Pleurotus ostreatus* extracts possess strong antioxidant properties in A549 cells, with increasing efficacy at higher concentrations.

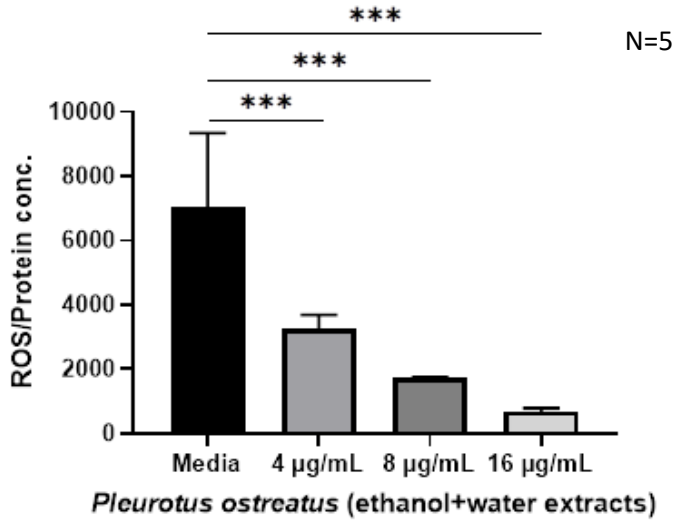

Figure 11. *Pleurotus Ostreatus* (ethanol + water extracts) in A549 monolayer culture. ROS/ Protein conc. plotted against Media, 4 µg/mL, 8 µg/mL, and 16 µg/mL conc. of *Pleurotus Ostreatus* (ethanol + water extracts).

The effect of *Ganoderma lucidum* (ethanol + water extracts) on ROS levels was assessed in A549 cells by measuring ROS normalized to protein concentration. As shown in Figure 12, the control group (Media) exhibited the highest ROS levels, exceeding 9000 ROS/protein concentration units. Treatment with *Ganoderma lucidum* extracts at 4 µg/mL, 8 µg/mL, and 16 µg/mL resulted in a significant reduction in ROS levels compared to the control. The 4 µg/mL and 8 µg/mL groups demonstrated a strong antioxidant effect, showing ROS levels reduced by more than half relative to the control The 16 µg/mL group exhibited the lowest ROS levels, suggesting a dose-

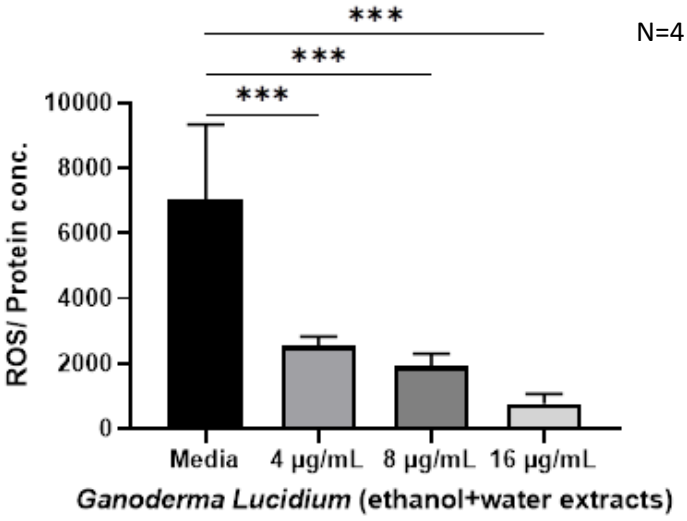

Figure 12. *Ganoderma lucidum* (ethanol + water extracts) in A549 monolayer culture. ROS/ Protein conc. plotted against Media, 4 µg/mL, 8 µg/mL, and 16 µg/mL conc. of *Ganoderma lucidum* (ethanol + water extracts).

dependent antioxidant response. Statistical analysis confirmed a highly significant reduction ($p < 0.001$) across all treatment groups. These results highlight the potent antioxidant properties of *Ganoderma lucidum* extracts in A549 cells, with maximum efficacy at 16 µg/mL.

Size determination of Spheroids

Depending on the number of cells seeded per well, the size of the spheroid varies. We observed that the maximum size that a spheroid can achieve is with a radius of 500 µm (Figure 13.a and c.). Increasing the cell number seeded per well increases the spheroid size until it reaches a radius of 500 µm at 1.5 × 10^4 cells per well. 2×10^4 cells caused the spheroid size to reduce and then gradually increase to the maximum size (Figure 13.c).To validate the formation of spheroids, we performed immunostaining. In a monolayer culture, cells spread and attach to the substrate, making the actin stress fibers elongated and when stained for E-cadherin, it is found to be localized at the cell-cell junction. On the contrary, when spheroids were stained (Figure 12.b.), actin fibers were localized around the boundary indicating that cell spreading is minimal. Lack of distinct cell-cell junction staining also indicates that what is formed is indeed a spheroid. Interestingly, the maximum size achieved size of a spheroid a radius of 500 µm.

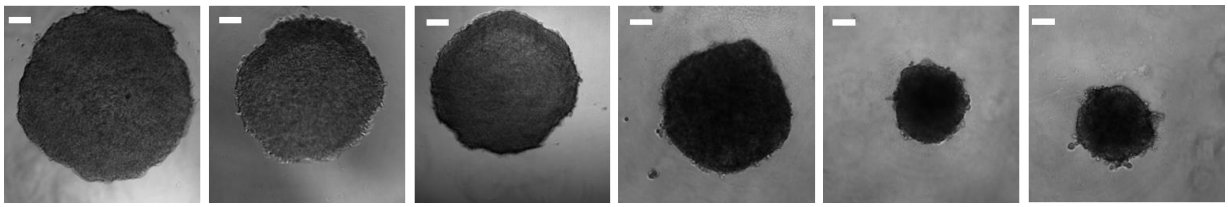

Figure 13.a. Varying sizes of Spheroids in correlation with the cells seeded per well.

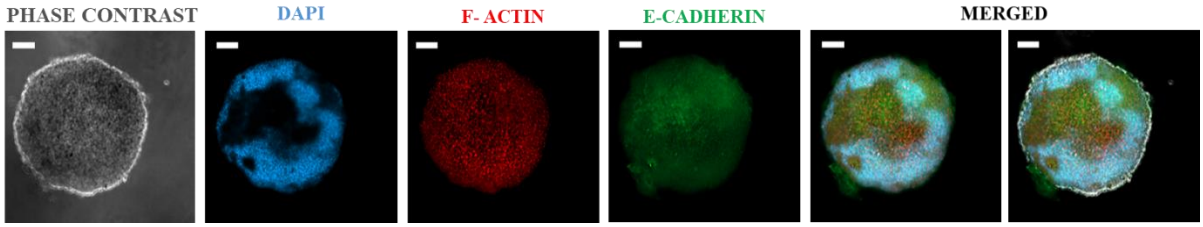

Figure 13.b. Staining spheroids to visualize stress fibers and cell-cell junction protein.

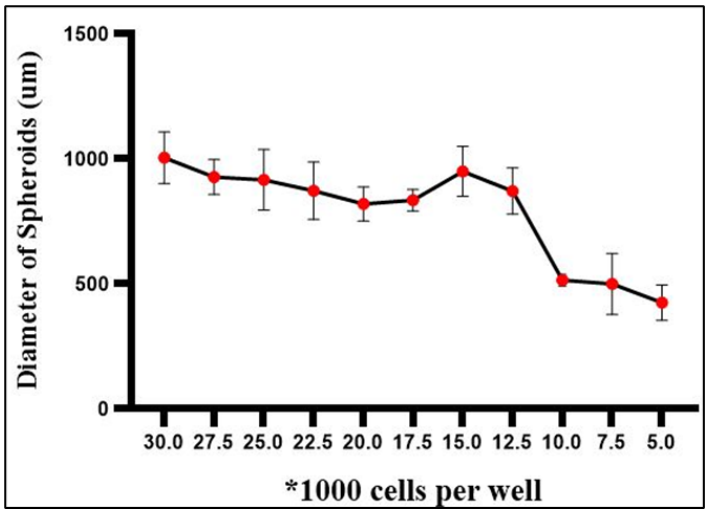

Figure. 13.c. Correlation between the number of cells seeded per well and the size of spheroids.

ROS in A549 Spheroids

A549 spheroids were treated with Mushroom extracts of *Pleurotus ostreatus* (ethanol + water extracts) and *Ganoderma lucidum* (ethanol + water extracts). ROS levels were measured and normalized to protein concentration. Spheroids were formed using 15,000, 20,000, 25,000, and 30,000 A549 cells per well and treated with increasing concentrations (4 µg/mL, 8 µg/mL, and 16 µg/mL) of both extracts (Figure 14. a, b, c, and d).

ROS levels in A549 spheroids treated with Pleurotus ostreatus extract

At 4 µg/mL, ROS levels are higher than the control (media-only spheroids). At 8 µg/mL, ROS levels were higher, especially in 20,000, 25,000, and 30,000-cell spheroids, indicating higher oxidative stress at this concentration. But at 16 µg/mL, ROS levels went down in cell densities across the sizes of spheroids, indicating that *Pleurotus ostreatus* could have an antioxidant effect at higher concentrations. The same trend was seen in all spheroid densities. This dual nature shows that at lower concentration, *Pleurotus ostreatus* may induce oxidative stress, but at higher concentration, it may play a protective role, perhaps through scavenging ROS.

ROS Levels of Ganoderma lucidum Treatments of A549 Spheroids

Another trend was observed for *Ganoderma lucidum* extract. At 4 µg/mL, ROS levels increased in the cell densities across the sizes of spheroids, similar to *Pleurotus ostreatus*. However, at 8 µg/mL, ROS levels were relatively constant in various sizes

of spheroids, rather than increasing as with *Pleurotus ostreatus*. At 16 µg/mL, ROS levels decreased, which indicates that *Ganoderma lucidum* is an antioxidant at higher concentrations as well. In comparison with *Pleurotus ostreatus*, which responded strongly to oxidative stress at 8 µg/mL, *Ganoderma lucidum* responded with a more consistent ROS profile before reducing at 16 µg/mL.

Effect of Spheroid Cell Count on ROS Quantity

Higher cell density in spheroids affected ROS production. Overall, spheroids seeded at higher cell densities (25,000 and 30,000 cells) had higher ROS at 8 µg/mL, indicating a greater oxidative response at higher cell densities. ROS, however, declined at all densities with 16 µg/mL, with the denser spheroids seeing a greater decline. This indicates that the oxidative stress response to these extracts can be affected by cell density.

Pleurotus ostreatus demonstrated an optimum ROS content at 8 µg/mL followed by a decline at 16 µg/mL, indicating an antioxidant effect depending on concentrations. *Ganoderma lucidum* had comparably stable ROS at 4 and 8 µg/mL, followed by a decrease at 16 µg/mL, suggesting a weak oxidative impact at low concentrations and an antioxidant impact at high concentrations. Increased cell densities were also seen to generate higher levels of ROS at 8 µg/mL but with more reduction at 16 µg/mL, indicating that cell density is involved in the oxidative stress response.

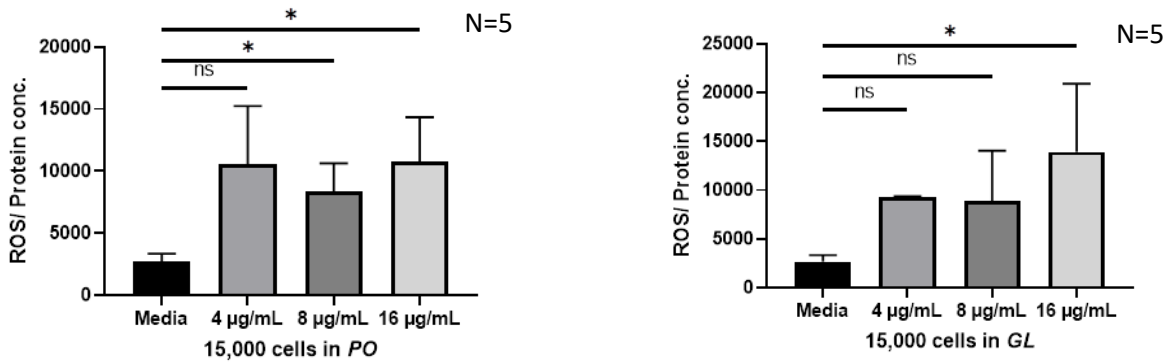

Figure 14.a. Reactive oxygen species (ROS) levels normalized to protein concentration in A549 spheroids seeded with 15,000 cells and treated with increasing concentrations (4 µg/mL, 8 µg/mL, and 16 µg/mL) of *Pleurotus ostreatus* (left) and *Ganoderma lucidum* (right) ethanol + water extracts. The control group (media)

represents untreated spheroids. Error bars indicate statistical significance. ns denotes no significant difference.

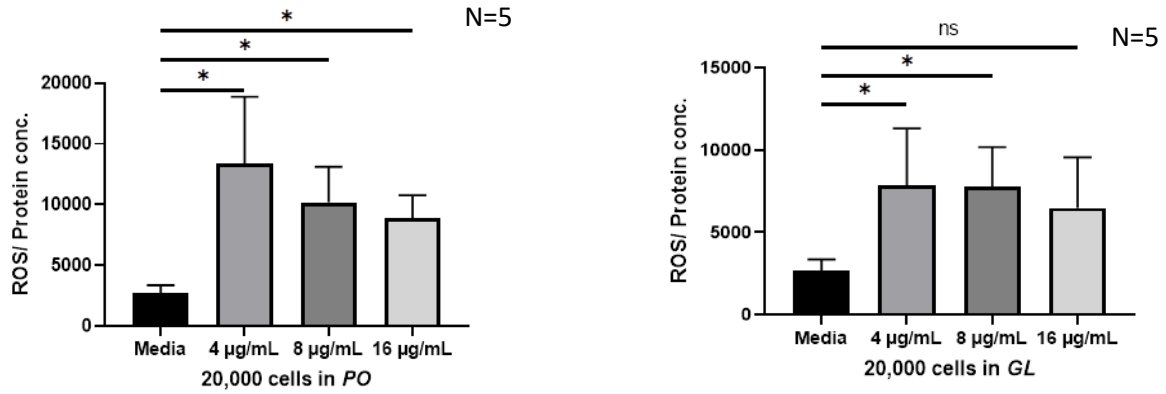

Figure 14.b. Reactive oxygen species (ROS) levels normalized to protein concentration in A549 spheroids seeded with 20,000 cells and treated with increasing concentrations (4 µg/mL, 8 µg/mL, and 16 µg/mL) of *Pleurotus ostreatus* (left) and *Ganoderma lucidum* (right) ethanol + water extracts. The control group (media) represents untreated spheroids. Error bars indicate statistical significance. ns denotes no significant difference.

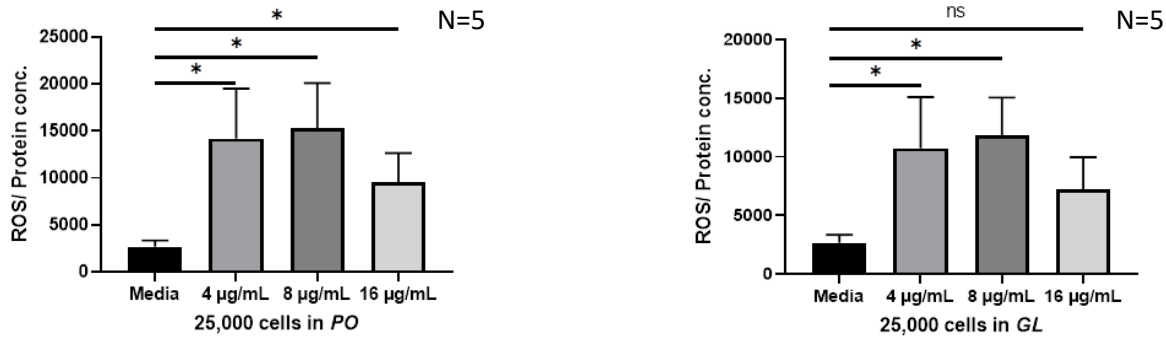

Figure 14.c. Reactive oxygen species (ROS) levels normalized to protein concentration in A549 spheroids seeded with 25,000 cells and treated with increasing concentrations (4 µg/mL, 8 µg/mL, and 16 µg/mL) of *Pleurotus ostreatus* (left) and *Ganoderma lucidum* (right) ethanol + water extracts. The control group (media) represents untreated spheroids. Error bars indicate statistical significance. ns denotes no significant difference.

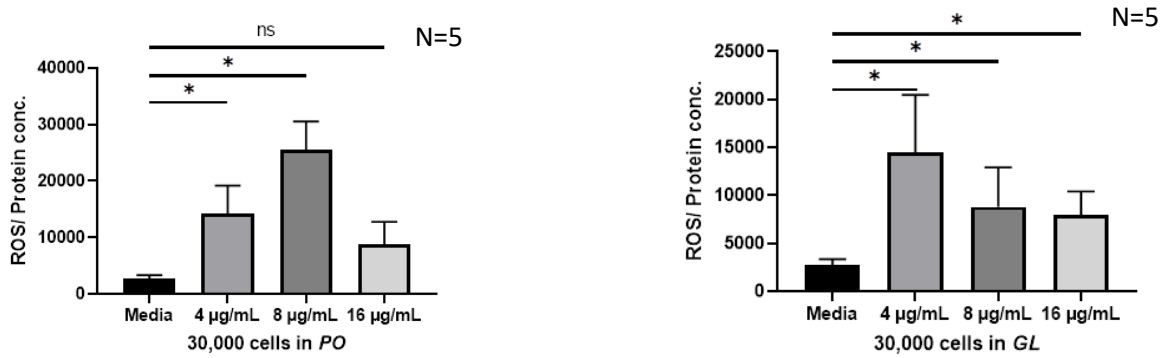

Figure 14.d. Reactive oxygen species (ROS) levels normalized to protein concentration in A549 spheroids seeded with 30,000 cells and treated with increasing concentrations (4 µg/mL, 8 µg/mL, and 16 µg/mL) of *Pleurotus ostreatus* (left) and *Ganoderma lucidum* (right) ethanol + water extracts. The control group (media) represents untreated spheroids. Error bars indicate statistical significance. ns denotes no significant difference.

GLUT 1 expression in A549

Western blotting was conducted to determine the level of GLUT1 expression in *Pleurotus ostreatus* and *Ganoderma lucidum* extract-treated A549 cells. Preliminary observations indicate potential variation in GLUT1 expression in different treatment groups demonstrated in Figure 15. However, as these are preliminary observations, further replicates and quantification must be conducted to validate these observations. No definitive conclusions can be drawn regarding the impact of these extracts on GLUT1 expression at this stage.

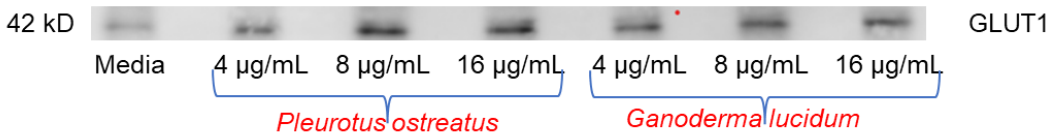

Figure 15. GLUT1 expression in A549 monolayer.

Chapter 4. Discussion

This study investigated the antioxidant activities of *Pleurotus ostreatus* and *Ganoderma lucidum* extracts against BEAS2B cells and A549 lung cancer cells and contrasted their activities within monolayer cultures and 3D spheroids. The results showed differential activities against the extracts, highlighting the use of spheroids in determining therapeutic efficacy.

In monolayer cultures, the two extracts lowered ROS levels in a dose-dependent fashion, with *Ganoderma lucidum* having the most significant lowering at 16 µg/mL. This is consistent with the established antioxidant activity of bioactive compounds such as phenolics, flavonoids, and polysaccharides that scavenges free radicals and boost cellular antioxidant defences. The uniform lowering of ROS levels addresses the possibility of these extracts in preventing oxidative stress in normal cellular contexts.

On the other hand, A549 spheroids demonstrated a significant increase in reactive oxygen species (ROS) levels following treatment with the extracts, particularly at higher concentrations. This can be explained by the complex tumor microenvironment inherent in spheroids, which includes regions of hypoxia, limitations in the availability of nutrients, and elevated metabolic activity. The extracts could disrupt redox balance in such a setting, forcing cancer cells to surpass their oxidative stress tolerance, thus initiating cell death. This specific effect is most easily seen in larger spheroids (25,000 and 30,000 cells), which by their nature have elevated basal ROS levels due to their compact structural composition.

The differential cell responses noted between monolayer and spheroid cultures suggest that the bioactive compounds *of Pleurotus ostreatus* and *Ganoderma lucidum* can act as antioxidants in healthy cell environments but pro-oxidants in cancerous environments. This biphasic effect is consistent with previous reports with respect to *Ganoderma lucidum*, where its triterpenoids and polysaccharides are said to be pro-oxidant at higher dosages, selectively targeting cancer cells for killing without damaging healthy cells.

The observed expression levels of GLUT1 in different extracts of mushrooms hints the role of major glucose transporters in cancer metabolism. Decreased GLUT1 expression can disrupt glycolytic flux, leading to increased oxidative stress and compromising the survival of cancer cells. How ROS modulation, GLUT1 expression,

and apoptosis pathways are interlinked should be investigated in the future to be able to fully understand the underlying mechanisms of such effects.

In summary, although *Pleurotus ostreatus* and *Ganoderma lucidum* extracts possess strong antioxidant activity in monolayer cultures, their capacity to cause oxidative stress in 3D spheroids defines their translational potential as anticancer drugs against lung cancer. The results define the significance of context-dependent effects and justify the conduct of additional *in vivo* studies to establish their translational potential in oxidative stress diseases and cancer therapy.

References

1. Sharma, Rajesh, and Jagdish Khubchandani. “Global, Regional, and National Burden of Tracheal, Bronchus, and Lung Cancer in 2022: Evidence from the GLOBOCAN Study.” *Epidemiologia*, vol. 5, no. 4, Dec. 2024, pp. 785–95. *DOI.org (Crossref)*, https://doi.org/10.3390/epidemiologia5040053.

2. Zhang, Xin, et al. “Disease Burden of Trachea, Bronchus and Lung Cancer 1990–2021 and Global Trends Projected to 2035.” Scientific Reports, vol. 15, no. 1, Feb. 2025, p. 6264. DOI.org (Crossref), https://doi.org/10.1038/s41598-025-90537-8.

3. Bizuayehu, Habtamu Mellie, et al. “Global Disparities of Cancer and Its Projected Burden in 2050.” *JAMA Network Open*, vol. 7, no. 11, Nov. 2024, p. e2443198. *DOI.org (Crossref)*, https://doi.org/10.1001/jamanetworkopen.2024.43198.

4. Van Den Boogaard, Winnie M. C., et al. “Chemotherapy Side-Effects: Not All DNA Damage Is Equal.” Cancers, vol. 14, no. 3, Jan. 2022, p. 627. DOI.org (Crossref), https://doi.org/10.3390/cancers14030627.

5. Cooper GM. The Cell: A Molecular Approach. 2nd edition. Sunderland (MA): Sinauer Associates; 2000. The Development and Causes of Cancer. Available from: https://www.ncbi.nlm.nih.gov/books/NBK9963/.

6. Joseph, Thomson Patrick, et al. “A Preclinical Evaluation of the Antitumor Activities of Edible and Medicinal Mushrooms: A Molecular Insight.” Integrative Cancer Therapies, vol. 17, no. 2, June 2018, pp. 200–09. DOI.org (Crossref), https://doi.org/10.1177/1534735417736861.

7. Zhang, Qing-Yu, et al. “Natural Product Interventions for Chemotherapy and Radiotherapy-Induced Side Effects.” Frontiers in Pharmacology, vol. 9, Nov. 2018, p. 1253. DOI.org (Crossref), https://doi.org/10.3389/fphar.2018.01253.

8. Meng, Xin, et al. “Antitumor Polysaccharides from Mushrooms: A Review on the Structural Characteristics, Antitumor Mechanisms and Immunomodulating Activities.” Carbohydrate Research, vol. 424, Apr. 2016, pp. 30–41. DOI.org (Crossref), https://doi.org/10.1016/j.carres.2016.02.008.

9. Wagh, Ha, et al. “The Effects of Different Substrates on the Nutritional Composition of Oyster Mushrooms (Pleurotus Sajor-Caju).” *International Journal of Fauna and*

Biological Studies, vol. 8, no. 2, Mar. 2021, pp. 98–101. *DOI.org (Crossref)*, https://doi.org/10.22271/23940522.2021.v8.i2b.817.

10. Bilal, Ahmad Wani, et al. “Nutritional and Medicinal Importance of Mushrooms.” *Journal of Medicinal Plants Research*, vol. 4, no. 24, Dec. 2010, pp. 2598–604. *DOI.org (Crossref)*, https://doi.org/10.5897/JMPR09.565.

11. “Nutritional and Medicinal Benefits of Oyster (Pleurotus) Mushrooms: A Review.” Fungal Biotec, vol. 1, no. 2, Jan. 2021, pp. 65–87. DOI.org (Crossref), https://doi.org/10.5943/FunBiotec/1/2/5.

12. Effiong, Magdalene Eno, et al. “Comparative Antioxidant Activity and Phytochemical Content of Five Extracts of Pleurotus Ostreatus (Oyster Mushroom).” Scientific Reports, vol. 14, no. 1, Feb. 2024, p. 3794. DOI.org (Crossref), https://doi.org/10.1038/s41598-024-54201

13. Barrett, Brendan J., and Patrick S. Parfrey. “Prevention of Nephrotoxicity Induced by Radiocontrast Agents.” New England Journal of Medicine, vol. 331, no. 21, Nov. 1994, pp. 1449–50. DOI.org (Crossref), https://doi.org/10.1056/NEJM199411243312111.

14. Kolniak-Ostek, Joanna, et al. “Anticancer and Antioxidant Activities in Ganoderma Lucidum Wild Mushrooms in Poland, as Well as Their Phenolic and Triterpenoid Compounds.” International Journal of Molecular Sciences, vol. 23, no. 16, Aug. 2022, p. 9359. DOI.org (Crossref), https://doi.org/10.3390/ijms23169359.

15. Averill-Bates, Diana. “Reactive Oxygen Species and Cell Signaling. Review.” Biochimica et Biophysica Acta (BBA) - Molecular Cell Research, vol. 1871, no. 2, Feb. 2024, p. 119573. DOI.org (Crossref), https://doi.org/10.1016/j.bbamcr.2023.119573.

16. Sies, Helmut, et al. “Defining Roles of Specific Reactive Oxygen Species (ROS) in Cell Biology and Physiology.” *Nature Reviews Molecular Cell Biology*, vol. 23, no. 7, July 2022, pp. 499–515. *DOI.org (Crossref)*, https://doi.org/10.1038/s41580-022-00456-z.

17. Sainero-Alcolado, Lourdes, et al. “Targeting Mitochondrial Metabolism for Precision Medicine in Cancer.” Cell Death & Differentiation, vol. 29, no. 7, July 2022, pp. 1304–17. DOI.org (Crossref), https://doi.org/10.1038/s41418-022-01022-y.

18. Hendrix, Sophie, et al. “Jack of All Trades: Reactive Oxygen Species in Plant Responses to Stress Combinations and Priming-Induced Stress Tolerance.” Journal

of Experimental Botany, Feb. 2025, p. eraf065. DOI.org (Crossref), https://doi.org/10.1093/jxb/eraf065.

19. Davydov, Dmitri R. “Microsomal Monooxygenase in Apoptosis: Another Target for Cytochrome c Signaling?” *Trends in Biochemical Sciences*, vol. 26, no. 3, Mar. 2001, pp. 155–60. *DOI.org (Crossref)*, https://doi.org/10.1016/S0968-0004(00)01749-7.

20. Nieto, Natalia, et al. “Stimulation and Proliferation of Primary Rat Hepatic Stellate Cells by Cytochrome P450 2E1-Derived Reactive Oxygen Species.” *Hepatology*, vol. 35, no. 1, Jan. 2002, pp. 62–73. *DOI.org (Crossref)*, https://doi.org/10.1053/jhep.2002.30362.

21. Galadari, Sehamuddin, et al. “Reactive Oxygen Species and Cancer Paradox: To Promote or to Suppress?” Free Radical Biology and Medicine, vol. 104, Mar. 2017, pp. 144–64. DOI.org (Crossref), https://doi.org/10.1016/j.freeradbiomed.2017.01.004.

22. Poirier, Yves, et al. “Peroxisomal β-Oxidation—A Metabolic Pathway with Multiple Functions.” *Biochimica et Biophysica Acta (BBA) - Molecular Cell Research*, vol. 1763, no. 12, Dec. 2006, pp. 1413–26. *DOI.org (Crossref)*, https://doi.org/10.1016/j.bbamcr.2006.08.034.

23. Rauf, Abdur, et al. “Reactive Oxygen Species in Biological Systems: Pathways, Associated Diseases, and Potential Inhibitors—A Review.” *Food Science & Nutrition*, vol. 12, no. 2, Feb. 2024, pp. 675–93. *DOI.org (Crossref)*, https://doi.org/10.1002/fsn3.3784.

24. Glorieux, Christophe, et al. “Targeting ROS in Cancer: Rationale and Strategies.” Nature Reviews Drug Discovery, vol. 23, no. 8, Aug. 2024, pp. 583–606. DOI.org (Crossref), https://doi.org/10.1038/s41573-024-00979-4.

25. Cheung, Eric C., and Karen H. Vousden. “The Role of ROS in Tumour Development and Progression.” *Nature Reviews Cancer*, vol. 22, no. 5, May 2022, pp. 280–97. *DOI.org (Crossref)*, https://doi.org/10.1038/s41568-021-00435-0.

26. He, Yan, et al. “Targeting PI3K/Akt Signal Transduction for Cancer Therapy.” *Signal Transduction and Targeted Therapy*, vol. 6, no. 1, Dec. 2021, p. 425. *DOI.org (Crossref)*, https://doi.org/10.1038/s41392-021-00828-5.

27. Thompson, Craig B., et al. “A Century of the Warburg Effect.” *Nature Metabolism*, vol. 5, no. 11, Nov. 2023, pp. 1840–43. *DOI.org (Crossref)*, https://doi.org/10.1038/s42255-023-00927-3.

28. Bao, Yang-Yang, et al. “Effect of Glut-1 and HIF-1α Double Knockout by CRISPR/CAS9 on Radiosensitivity in Laryngeal Carcinoma via the PI3K/Akt/mTOR Pathway.” *Journal of Cellular and Molecular Medicine*, vol. 26, no. 10, May 2022, pp. 2881–94. *DOI.org (Crossref)*, https://doi.org/10.1111/jcmm.17303.

29. Deng, Huan, et al. “PI3K/AKT/mTOR Pathway, Hypoxia, and Glucose Metabolism: Potential Targets to Overcome Radioresistance in Small Cell Lung Cancer.” *Cancer Pathogenesis and Therapy*, vol. 1, no. 1, Jan. 2023, pp. 56–66. *DOI.org (Crossref)*, https://doi.org/10.1016/j.cpt.2022.09.001.

30. Jeyaraj, Ethel Jeyaseela, et al. “Effect of Organic Solvents and Water Extraction on the Phytochemical Profile and Antioxidant Activity of *Clitoria Ternatea* Flowers.” *ACS Food Science & Technology*, vol. 1, no. 9, Oct. 2021, pp. 1567–77. *DOI.org (Crossref)*, https://doi.org/10.1021/acsfoodscitech.1c00168.

31. Adaramola, Feyisara, et al. “Assessment of Phytochemicals, Antioxidant and Antimicrobial Activities of Aqueous Ethanol Extract and Fractions of Azadirachta Indica Stem Bark.” *International Journal of Science for Global Sustainability*, vol. 9, no. 1, Dec. 2021, p. 13. *DOI.org (Crossref)*, https://doi.org/10.57233/ijsgs.v9i1.401.

32. Zhang, Xin, et al. “Disease Burden of Trachea, Bronchus and Lung Cancer 1990–2021 and Global Trends Projected to 2035.” *Scientific Reports*, vol. 15, no. 1, Feb. 2025, p. 6264. *DOI.org (Crossref)*, https://doi.org/10.1038/s41598-025-90537-8.